IEEE Access
Multidisciplinary | Rapid Review | Open Access Journal

SPECIAL SECTION ON EMERGING TRENDS, ISSUES AND CHALLENGES IN UNDERWATER ACOUSTIC SENSOR NETWORKS

Received May 5, 2019, accepted May 16, 2019, date of publication May 27, 2019, date of current version June 10, 2019.

Digital Object Identifier 10.1109/ACCESS.2019.2919346

Fault-Tolerant Prescribed Performance Control Algorithm for Underwater Acoustic Sensor Network Nodes With Thruster Saturation

HONGDE QIN[1], ZHEYUAN WU[1], YANCHAO SUN[1], CHAO ZHANG[2], AND CHUAN LIN[1,3]

[1]Science and Technology on Underwater Vehicle Laboratory, Harbin Engineering University, Harbin 150001, China
[2]Department of Control Science and Engineering, Harbin Institute of Technology, Harbin 150001, China
[3]Key Laboratory for Ubiquitous Network and Service Software of Liaoning province, School of Software, Dalian University of Technology, Dalian 116024, China

Corresponding author: Yanchao Sun (sunyanchao@hrbeu.edu.cn)

This work was supported in part by the National Natural Science Foundation of China under Grant U1713205 and Grant 61803119, and in part by the Research Fund from Science and Technology on Underwater Vehicle Technology, under Grant 6142215180208 and 6142215180101.

ABSTRACT This paper designs a prescribed performance fault-tolerant control strategy for the underwater acoustic sensor network nodes (UASNN) trajectory tracking control in the presence of ocean current disturbances, modeling uncertainties, and thruster faults. By using a general uncertainties observer, the influence of disturbances and uncertainties are estimated. Additionally, a novel performance function which determines explicitly the maximum convergence time is utilized. Based on the new performance function and corresponding error transformation, the 6-DOF tracking errors are restricted to prescribed bounds to ensure the desired transient and steady response. Furthermore, when considering thruster saturation, we introduce an auxiliary system to compensate for the saturation. The closed-loop system stability is proved by Lyapunov theory. The numerical simulations for three thruster faults are carried out to demonstrate that the proposed strategy is effective.

INDEX TERMS Underwater acoustic sensor networks, trajectory tracking control, prescribed performance, thruster fault, saturation.

I. INTRODUCTION

The ocean contains rich undiscovered natural resources, which include marine lives, mineral resources, and energy. In order to acquire the resources, people must master the key technologies, which contain the deep-sea navigation, exploration, and exploitation [1]–[5]. Using underwater acoustic sensor networks (UASNs) can obtain the information about changes in the marine environment more effectively, which is significantly important to marine resource exploration and scientific research [6]. A typical UASN employs underwater nodes, surface sinks, autonomous underwater vehicles and low-power gliders to collaboratively perform underwater operating missions [7]. Autonomous Underwater Vehicles (AUVs) usually are required in the sparse UASNs for implementing underwater surveillance or acting as message ferries [8], [9].

The associate editor coordinating the review of this manuscript and approving it for publication was Guangjie Han.

According to this background, an underwater acoustic sensor network node (UASNN) can be designed to widen out the UASNs [10]. The UASNN which combines advantages of fixed node and AUV can realize the autonomous deployment, accurate positioning, and data acquisition. Not only do they deploy rapidly to save time, especially in large-scale and transferable deployment, but you can also use them to replace faulted fixed node in traditional UASNs.

Given the fact that ocean data acquisition needs the large-scale UASNNs deploying simultaneously, the control system should not only overcome disturbances from the complicated ocean environment so that they can track desired trajectory to complete the deployment, but also improve control convergence process of tracking errors to avoid the collision risk in mass deployment. Modeling uncertainties and ocean current disturbances are common influence factors in trajectory tracking control for AUVs. As a special AUV, the UASNN also considers the influences caused by above factors. Observers and neural networks are often used to

deal with external disturbances [11], [12]. Reference [13] proposed an under-actuated AUV robust control scheme with modeling uncertainties and environmental disturbances. This method adopted an adaptive fuzzy control algorithm and a sliding-mode control approach to compensate for modeling uncertainties and disturbances, respectively. Reference [14] developed a robust control scheme based on terminal sliding-mode control methods to overcome the influence of uncertainties and disturbances. Reference [15] used radial basis function neural networks to approximate the nonlinear uncertainties and enhance the robustness of the AUV against the uncertainties and disturbances. Reference [16] designed a second-order sliding-mode control strategy which was comprised of an equivalent controller and a switching controller. The control algorithm could suppress the parameter uncertainties and eliminate the unpredictable disturbance effects caused by ocean currents. Reference[17] proposed an adaptive output feedback control approach and introduced an observer to reconstruct the full states. This method could make AUV track desired target in external disturbances. Reference [18] developed an adaptive fuzzy PI sliding-mode control strategy based on approximately known inverse dynamic model output while the continuous adaptive PI term overcame the influence of disturbances and uncertainties.

The above references contained many trajectory tracking control strategies to deal with the uncertainties and disturbances and obtained some good effects. However, these control strategies were designed under fault-free assumptions. Owing to the complexity of underwater environment, faults may occur in several components of the AUV, especially in thruster. Since the UASNNs are applied to large-scale deployment, thruster faults are worth considering. Reference [19] proposed a fault isolation issue for the redundant thrusters. This approach got rid of some fault-free terms from the given control input equations, and adopted consistency check to achieve control task. Reference [20] developed a novel fault detection observer with a non-singular structure. Reference [21] proposed a control technique based on fault-tolerant decomposition for thruster force allocation to deal with thruster fault for redundant-thruster AUV system. Reference [22] developed an improved Elman neural network which had stronger identification ability when applied to the AUV. This strategy calculated and analyzed the residual by comparing the model output with the actual measured values based on fault judging criteria to obtain fault diagnosis results. Reference [23] proposed a distributed fault-tolerant controller with the feedback of the information of rigid bodies only based on the sign function. Reference [24] combined infinity-norm optimization with 2-norm optimization for the optimal allocation of thrust to construct a bi-criteria primal-dual neural network fault-tolerant control method, and enhanced the robustness with respect to nonlinear characteristics for ROV. It is obvious that design ideas of above references were to design the fault diagnosis schemes separately. Reference [25] proposed an adaptive terminal sliding-mode fault-tolerant control technique, and introduced the adaptive strategy to estimate the upper bounds of the system general uncertainties which included uncertainties, disturbances, and thruster faults. Therefore, this strategy could handle the thrust faults more flexibly so that it is more suitable to be utilized when designing the fault-tolerant control schemes for the UASNNs.

The references mentioned gave the corresponding methods to deal with disturbances, uncertainties as well as thruster faults, and made the systems have certain stability and robustness. However, according to the UASNN special work requests which include large-scale deployment, high accuracy tracking, and landing on the seabed, we should not only consider the influence caused by above factors but also make trajectory tracking system have desired performance. Additionally, the overshoots also need to be limited to avoid hitting each other or other objects. In 2008, Bechlioulis proposed a prescribed performance control method, which introduced performance function and corresponding error transformation to make convergence rate, overshoot, and tracking error to obtain pre-established performances [26]. This algorithm was initially used to general nonlinear systems research. The prescribed performance method gradually extends to many other fields in recent years, such as chaotic system [27],[28], spacecraft system [29],[30], electro hydraulic system [31], and marine system [32]. According to the high performance of prescribed performance approach, we can introduce it into trajectory tracking control system of the UASNN.

The thruster saturation is a common problem which influences control effects in actual AUV systems. If the thruster saturation is ignored, it would bring adverse effects, such as reducing the system tracking precision or making the system instability. Reference [33] designed an L_1 adaptive control architecture with anti-windup to guarantee the robustness of the AUV with input saturation. Reference [34] proposed an adaptive control approach which combined a model reference adaptive algorithm, an integral state feedback, and a modern anti-windup compensator to accomplish adaptive autopilot in the presence of input saturations. Reference [35] developed an adaptive PID control method with a dynamic anti-windup compensator for AUVs to improve the quality of the adaptive controller when the saturation occurred. Reference [36] proposed an adaptive control strategy based on Lyapunov theory and the backstepping technique. This algorithm used saturation functions to bound control signals, and designed another adaptive strategy to deal with actuator saturation.

When considering disturbances, uncertainties, thruster faults, and thruster saturation, we propose a prescribed performance control method based on the general uncertainties observer for the trajectory tracking control of the UASNN. Firstly, we design a new performance function which can pre-establish convergence time of the tracking error. By utilizing the new function and corresponding error transformation, the trajectory tracking system of the UASNN is transformed into an equivalent error system to accomplish desired dynamic process with steady state response. Additionally, the general uncertainties observer is designed to estimate the

influence of disturbances, uncertainties, and thruster faults. When thruster saturation occurs, an auxiliary system is introduced to compensate the saturation. Finally, we use the Lyapunov theory to prove the stability of the closed-loop system. The simulation result indicates that the proposed control approach can effectively deal with the influence of above factors to obtain prescribed performance, even if the thruster saturation arises. In comparison with the existing works, the main contributions of this study are presented as follows:

1. In order to satisfy the high control requirements which includes to control convergence process of tracking errors and to have high precise of steady-state trajectory tracking for the UASNN, we use the prescribed performance algorithm to design the tracking control strategy to achieve desired control objectives.

2. This study introduces a new performance function which can pre-establish convergence time to overcome the problem, while the traditional performance function lacks a clear indication of actual convergence time [26], [44]. As a result, it is easier to be used in engineering practice.

3. The considerations for influence factors including ocean current disturbances, modeling uncertainties, thruster faults, and thruster saturation are not comprehensive and systematic in published references [13]–[17]. In this study, we design a general uncertainties observer and a saturation auxiliary system to solve them. Among them, the proposed observer can approximate the general uncertainties caused by external disturbances and thruster faults.

The remainder of this paper is organized as follows. Section II presents modeling and simplified process of the UASNN dynamic model. Section III introduces prescribed performance method and model transformation. The design process of the general uncertainties observer, saturation auxiliary system, and prescribed performance trajectory tracking controller is illustrated in Section IV. Section V shows the corresponding simulation results for different types of thruster faults and desired trajectories.

II. DESCRIPTION AND DYNAMIC MODEL OF THE UASNN

This study proposes a half open-frame UASNN model for the special design demands, which includes strong autonomy, precise positioning, and long-term operation for the ocean bottom data acquisition. The design of the UASNN is shown in Figure 1. The designed solution of UASNN adopts redundantly actuated configuration to resist ocean current to achieve dynamic positioning and landing on the seafloor. Additionally, the redundantly actuated model effectively promotes the system reliability to avoid serious influence caused by single thruster fault.

The dynamic model of the UASNN is the same as the traditional AUV nonlinear model. We introduce the 6 DOF AUV model with disturbances to represent dynamic model of the UASNN, as shown below [37]:

$$\dot{v} = M^{-1}\left[B_0 u - C_0(v)v - D_0(v)v - g_0(\eta)\right] - F \tag{1}$$

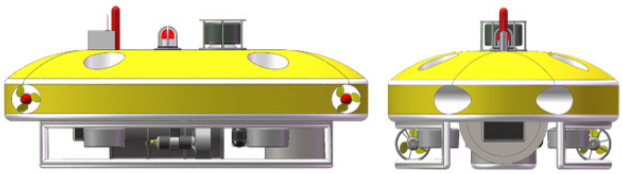

FIGURE 1. The half open-frame UASNN model.

$$F = M_0^{-1}(\Delta M\dot{v} - \Delta Bu + \Delta C(v)v + \Delta D(v)v + \Delta g(\eta) + \overline{C_{A\eta}\eta_r + D_\eta\eta_r}) \tag{2}$$

where F denotes system general uncertainties, subscript '0' and Δ represent the nominal and uncertain values of the corresponding variable, respectively. $v = [u, v, w, p, q, r]^{\mathrm{T}}$ denotes the velocity and angular velocity vector of the UASNN in the body-fixed frame. M is the inertia matrix of the UASNN. $\eta = [x, y, z, \phi, \theta, \psi]^{\mathrm{T}}$ represents position and attitude vector in the inertial frame. B_0 denotes nominal value of the thrust allocation matrix, u represents control output of the thrusters. $C(v)$, $D(v)$, and $g(\eta)$ represent the coriolis and centripetal matrix, damping matrix, and vector of gravitational/buoyancy forces and moments, respectively. $\overline{C_{A\eta}\eta_r + D_\eta\eta_r}$ is the influence of ocean current disturbances. η_r is the vehicle position and orientation vector relative to ocean current. $\Delta B = KB_0$ denotes the thrust allocation matrix which is influenced by thruster faults, and K is a diagonal matrix while the element $k_{ii} \in [0, 1]$, which represents the level of the corresponding thruster fault [38]. We can conclude that the ocean current disturbances, modeling uncertainties, and thruster faults can be compounded and act on the dynamic model of the UASNN together with the control force. This strategy could handle those disturbances more flexibly so that it is more suitable to be utilized when designing the system disturbance observer for the UASNNs.

To simplify, we propose two assumptions based on practical project background.

Assumption 1: The position and attitude vector η and the velocity and angular velocity vector v are available for measurement.

Assumption 2: The desired position and attitude vector η_d and its first and second derivatives are known bounded functions.

III. THE PRESCRIBED PERFORMANCE ALGORITHM

A. THE DEFINITION OF PERFORMANCE FUNCTION

In order to accomplish prescribed performance control, we introduce performance function as pre-established error boundary. Firstly, the definition of performance function is given as follow:

Definition 1: A smooth function $\rho(t)$: $\mathrm{R}_+ \rightarrow \mathrm{R}$ can be called a performance function if

1. $\rho(t)$ is decreasing and positive.
2. $\lim_{t\to\infty} \rho(t) = \rho_\infty > 0$.

The common performance function is shown as follows.

$$\rho(t) = (\rho_0 - \rho_\infty) e^{-kt} + \rho_\infty \tag{3}$$

where ρ_0, ρ_∞ and k are preset positive constants.

The tracking error by using the performance function can be rewritten as follow

$$\begin{aligned} -\delta_i \rho_i(t) < e_i(t) < \rho_i(t), e_i(0) \geq 0; \\ -\rho_i(t) < e_i(t) < \delta_i \rho_i(t), e_i(0) < 0. \end{aligned} \tag{4}$$

where $e_i(t), i = 1, 2, 3, 4, 5, 6$ is position and attitude error of the UASNN, and $0 \leq \delta_i \leq 1$. According to the performance function (3) and Eq.(4), k and ρ_∞ limits minimum convergence rate of tracking error and defines the upper boundary of steady state error, respectively, if the initial value of tracking error satisfies $0 \leq \|e_i(0)\| \leq \rho_i(0)$. Therefore, we can design proper performance function $\rho_i(t)$ and parameter δ_i to obtain desired objectives.

It is obvious that the convergence rate of the traditional performance function (3) depends on exponential term e^{-kt}. The exponential form is difficult to build a clear mathematical relationship between constant k and actual convergent speed. Additionally, the choice of the constant k has no specific rule. Therefore, **we design a new performance function.**

$$\rho(t) = \begin{cases} a_1 + a_2 \sin\left(\frac{\pi t}{2t_f}\right) + a_3 \cos\left(\frac{\pi t}{2t_f}\right) + a_4 e^{-kt}, & 0 \leq t \leq t_f \\ \rho_{tf} & t > t_f \end{cases} \tag{5}$$

where a_1, a_2, a_3, and a_4 are design parameters. k and $\rho_{tf} = \rho_\infty$ are the same with traditional performance function (3). The parameter t_f defines the terminal time at which performance function (5) reaches ρ_∞. We make Eq.(5) accord with define 1 via two steps.

Step 1: Select suitable parameters a_1, a_2, a_3, and a_4.

The initial and terminal conditions of the new performance function (5) are the same as the traditional function (3). The conditions can be expressed as $\rho(0) = \rho_0$ and $\rho(t_f) = \rho_{tf}$, where the first and second derivatives of $\rho(t)$ with respect to time are continuous functions. Thus we demand that $\lim_{t \to t_f^-} \dot{\rho}(t) = \lim_{t \to t_f^+} \dot{\rho}(t) = 0$ and $\lim_{t \to t_f^-} \ddot{\rho}(t) = \lim_{t \to t_f^+} \ddot{\rho}(t) = 0$. The four unknown parameters a_1, a_2, a_3, and a_4 can be calculated based on above conditions. Let $a_0 = 2t_f k/\pi$, we can obtain

$$\begin{aligned} a_1 &= \rho_0 + (a_0 e^{-kt_f} - 1) a_4 \\ a_2 &= a_0^2 a_4 e^{-kt_f} \\ a_3 &= -a_0 a_4 e^{-kt_f} \\ a_4 &= \frac{\rho_0 - \rho_{t_f}}{1 - (a_0^2 + a_0 + 1) e^{-kt_f}} \end{aligned} \tag{6}$$

Step.2: Verify that $\rho(t)$ is a monotonic decreasing and positive function.

Since $\rho(0) = \rho_0 > 0$ and $\rho(t_f) = \rho_{t_f} > 0$, $\rho(t)$ satisfies the monotonic decreasing and positive conditions if $\dot{\rho}(t) < 0$ is true for $t \in [0, t_f)$.

Proof [39]: Take the derivative of Eq. (5) with respect to time and substitute the values of a_0, a_1, a_2, a_3, and a_4 into it

$$\begin{aligned} \dot{\rho}(t) &= a_2 \frac{\pi}{2t_f} \cos\left(\frac{\pi}{2t_f}\right) - a_3 \frac{\pi}{2t_f} \sin\left(\frac{\pi t}{2t_f}\right) - k a_4 e^{-kt} \\ &= \frac{2t_f k^2}{\pi} a_4 e^{-kt_f} \cos\left(\frac{\pi t}{2t_f}\right) + k a_4 e^{-kt_f} \sin\left(\frac{\pi t}{2t_f}\right) \\ &\quad - k a_4 e^{-kt}, 0 \leq t \leq t_f \end{aligned} \tag{7}$$

As is known from the calculation, $k a_4 > 0$. Therefore, the original problem can be transformed into the case that confirming whether $y < 0$ in interval $[0, t_f)$ can be established, where

$$\begin{aligned} y = \frac{2t_f k}{\pi} e^{-kt_f} \cos\left(\frac{\pi t}{2t_f}\right) + e^{-kt_f} \frac{\pi}{2t_f} \sin\left(\frac{\pi t}{2t_f}\right) \\ - e^{-kt}, 0 \leq t \leq t_f \end{aligned} \tag{8}$$

Let $c = t_f k$ and $x = t/t_f$. Eq.(8) can be rewritten as

$$y = \frac{2}{\pi} c \cdot \cos\left(\frac{\pi}{2} x\right) + \sin\left(\frac{\pi}{2} x\right) - e^{c(1-x)}, 0 \leq x \leq 1 \tag{9}$$

And now we have to take the first and second derivatives of $y(x)$ with respect to x based on the initial values of $y(x)$ and $\dot{y}(x)$ including $y(0) = 2c/\pi - e^c < 0$, $y(1) = 0$, $\dot{y}(0) = \pi/2 + c e^c > 0$, and $\dot{y}(1) = 0$.

$$\dot{y}(x) = -c \sin\left(\frac{\pi}{2} x\right) + \frac{\pi}{2} \cos\left(\frac{\pi}{2} x\right) + c e^{c(1-x)}, 0 \leq x \leq 1 \tag{10}$$

$$\begin{aligned} \ddot{y}(x) = -\frac{\pi}{2} c \cdot \cos\left(\frac{\pi}{2} x\right) - \frac{\pi^2}{4} \sin\left(\frac{\pi}{2} x\right) \\ - c^2 e^{c(1-x)}, 0 \leq x \leq 1 \end{aligned} \tag{11}$$

It is obvious that $\ddot{y}(x) < 0$, that is, $\dot{y}(x)$ is a monotone decreasing function. On account of $\dot{y}(0) > 0$ and $\dot{y}(1) = 1$, we know that $\dot{y}(x) \geq 0$ in interval $[0, 1]$, and $y(x)$ is a monotone increasing function. $y(x) \leq 0$ since $y(0) < 0$ and $y(1) = 0$. Therefore, $\dot{\rho}(t) < 0$ for all $0 \leq t \leq t_f$ ($\dot{\rho}(t) = 0$ if and only if $t = t_f$), that means, $\rho(t)$ is a monotone decreasing and positive function.

Hence, Eq.(5) is a performance function where the setting of corresponding parameters is given in Eq.(6). The step 2 demonstrates that the selection of parameters t_f and k affects the convergence speed of the performance function (5), and they can be chosen without constraints. The new performance function (5) has the following important properties:

1. The maximum convergence time t_f can be pre-established.

2. When the steady state convergence time is given, we can adjust parameter k to change the convergent speed of the performance function (5).

Remark 1: On account of traditional performance function (3) which adopts exponential convergence form, the convergent speed depends on the parameter k. The traditional performance function is difficult to satisfy requirements when we

hope to reduce the initial convergent speed to avoid overlarge control demand. The proposed new performance function (5) can choose appropriate parameter t_f to ensure the system convergence within desired time, and adjust parameter k to control initial convergent speed of the error system.

B. ERROR TRANSFORMATION

In order to solve prescribed performance control problem satisfying Eq.(4), we introduce an error transformation to transform the tracking control system with the constraint into an equivalent unconstrained one. We define a function $S_i(\varepsilon_i)$ which has the following properties:

(1) $S_i(\varepsilon_i)$ is a smooth and monotonic increasing function.

(2)

$$-\delta_i < S_i(\varepsilon_i) < 1, e_i(0) \geq 0$$
$$-1 < S_i(\varepsilon_i) < \delta_i, e_i(0) < 0;$$

(3)

$$\left.\begin{array}{l}\lim\limits_{\varepsilon_i \to -\infty} S_i(\varepsilon_i) = -\delta_i \\ \lim\limits_{\varepsilon_i \to +\infty} S_i(\varepsilon_i) = 1\end{array}\right\}, e_i(0) \geq 0,$$
$$\left.\begin{array}{l}\lim\limits_{\varepsilon_i \to -\infty} S_i(\varepsilon_i) = -1 \\ \lim\limits_{\varepsilon_i \to +\infty} S_i(\varepsilon_i) = \delta_i\end{array}\right\}, e_i(0) < 0$$

where $\varepsilon_i \in (-\infty, +\infty)$ is the transformed error. An acceptable function $S_i(\varepsilon_i)$ is shown as follow:

$$S_i(\varepsilon_i) = \begin{cases} \dfrac{e^{\varepsilon_i} - \delta_i e^{-\varepsilon_i}}{e^{\varepsilon_i} + e^{-\varepsilon_i}}, e_i(0) \geq 0; \\ \dfrac{\delta_i e^{\varepsilon_i} - e^{-\varepsilon_i}}{e^{\varepsilon_i} + e^{-\varepsilon_i}}, e_i(0) < 0; \end{cases} \tag{12}$$

Based on $S_i(\varepsilon_i)$, Eq. (4) can be equivalently expressed as

$$e_i(t) = \rho_i(t) S_i(\varepsilon_i) \tag{13}$$

Owing to the monotone increasing property of $S_i(\varepsilon_i)$, the inverse function must exist.

$$\varepsilon_i = S_i^{-1}\left(\frac{e_i(t)}{\rho_i(t)}\right) \tag{14}$$

If we can keep ε_i bounded, then Eq.(4) holds, so that the tracking error could obtain desired control objectives under the constraint of performance function. Therefore, the tracking control problem of system (1) is transformed into a stabilization control of closed-loop system with respect to ε_i.

The $S_i(\varepsilon_i)$ can be described as Eq.(12), then

$$\varepsilon_i = S_i^{-1}\left(\frac{e_i(t)}{\rho_i(t)}\right) = \begin{cases} \frac{1}{2}\ln\dfrac{z_i + \delta_i}{1 - z_i}, e_i(0) \geq 0; \\ \frac{1}{2}\ln\dfrac{1 + z_i}{\delta_i - z_i}, e_i(0) < 0; \end{cases} \tag{15}$$

where $z_i = e_i(t)/\rho_i(t)$.

Remark 2: When $e_i(0) = 0$, δ_i cannot be chosen as zero based on Eq.(15), since it will make the initial value of transformed error be infinity.

We take a derivative of ε_i with respect to time.

$$\dot{\varepsilon}_i = \frac{\partial S_i^{-1}}{\partial z_i} \cdot \dot{z}_i = \frac{\partial S_i^{-1}}{\partial z_i} \cdot \frac{\dot{e}_i\rho_i - e_i\dot{\rho}_i}{\rho_i \cdot \rho_i} = r_i\left(\dot{e}_i - \frac{e_i\dot{\rho}_i}{\rho_i}\right) \tag{16}$$

where $r_i = \left(\partial S_i^{-1}/\partial z_i\right) \cdot (1/\rho_i)$ can be calculated by Eq.(15). On account of $\left(\partial S_i^{-1}/\partial z_i\right) > 0$ and $\rho_i(t) > 0$, we know $r_i > 0$. Additionally, r_i is bounded if the error $e_i(t)$ strictly satisfies Eq.(4), that is, $r < r_i < r''$, and r'' is a positive constant.

Take the second derivative of ε_i with respect to time.

$$\begin{aligned}\ddot{\varepsilon}_i &= \dot{r}_i(\dot{e}_i - \frac{e_i\dot{\rho}_i}{\rho_i}) + r_i(\ddot{e}_i - \frac{\dot{e}_i\dot{\rho}_i\rho_i + e_i\ddot{\rho}_i\rho_i + e_i\dot{\rho}_i^2}{\rho_i^2}) \\ &= \dot{r}_i(\dot{e}_i - \frac{e_i\dot{\rho}_i}{\rho_i}) - r_i \cdot \frac{\dot{e}_i\dot{\rho}_i\rho_i + e_i\ddot{\rho}_i\rho_i + e_i\dot{\rho}_i^2}{\rho_i^2} + r_i(\ddot{\eta}_i - \ddot{\eta}_{di})\end{aligned} \tag{17}$$

where $\ddot{\eta}_i, \ddot{\eta}_{di}$ $(i = 1, 2, 3, 4, 5, 6)$ represent the second derivatives of actual and desired trajectories, respectively.

The error variable $s \in \mathrm{R}^6$ can be written as

$$s = \lambda\varepsilon + \dot{\varepsilon} \tag{18}$$

where $\varepsilon = [\varepsilon_1, \varepsilon_2, \varepsilon_3, \varepsilon_4, \varepsilon_5, \varepsilon_6]^{\mathrm{T}}$ and $\lambda = \mathrm{diag}[\lambda_1, \lambda_2, \lambda_3, \lambda_4, \lambda_5, \lambda_6]$ 0 are design parameters. According to the dynamic model (1) of the UASNN, Eq.(18) can be rewritten as

$$\dot{v} = M^{-1}\left[B_0 u - C_{v0}v - D_{v0}v - g_{\eta 0}\right] - F.$$

It can be rewritten as

$$\begin{aligned}\ddot{\eta}_e &= \dot{J}(\eta)v_e + J(\eta)\dot{v}_e \\ &= \dot{J}(\eta)v_e + J(\eta)[M_0^{-1}(B_0 u - C_{v0}v \\ &\qquad - D_{v0}v - g_{\eta 0}) - F] - J(\eta)\dot{v}_d\end{aligned} \tag{19}$$

where $\ddot{\eta}_e = \ddot{\eta} - \ddot{\eta}_d$, $v_e = v - v_d$, and $\dot{v}_e = \dot{v} - \dot{v}_d$. J denotes the transformation matrix between the inertial frame and the body-fixed frame. Let $G = \dot{J}(\eta)v_e - J(\eta)M_0^{-1}(B_0 u + C_{v0}v + D_{v0}v + g_{\eta 0}) - J(\eta)\dot{v}_d$, $H = J(\eta)M_0^{-1}B_0$, and $D = -J(\eta)F$. The Eq.(19) can be abbreviated as follow:

$$\ddot{\eta}_e = G + Hu + D \tag{20}$$

Then

$$\dot{s} = \lambda\dot{\varepsilon} + \ddot{\varepsilon} = V + R(G + Hu + D) \tag{21}$$

where $V = [v_1, v_2, v_3, v_4, v_5, v_6]^{\mathrm{T}}$, $v_i = \left(\lambda_i r_i + r''\right)$, $R = \mathrm{diag}[r_1, r_2, r_3, r_4, r_5, r_6]$. If we design controller u to make s bounded, ε_i and $\dot{\varepsilon}$ will all be bounded based on Eq.(18).

IV. PRESCRIBED PERFORMANCE CONTROLLER DESIGN WITH THRUSTER SATURATION

Thruster saturation must exist in actual systems. It is obvious that thruster is easier to reach saturation when control system obtains better control results. Therefore, in order to achieve desired control performance, it is worth to investigate the

design of trajectory tracking controller when considering the thruster saturation.

We use variable u_c to replace original control variable u when thruster saturation occurs. Then $u_c = sat(u) = [sat(u_1), sat(u_2), sat(u_3), sat(u_4), sat(u_5), sat(u_6)]^{\mathrm{T}}$, where u_c represents actual output value of the thrusters, and $sat(u_i) = \min\{|u_i|, u_{i\max}\} \cdot sgn(u_i)$, where $u_{i\max}$ represents the maximum output value of each axis. Then, the error system can be rewritten as

$$\dot{s} = \lambda\dot{\varepsilon} + \ddot{\varepsilon} = V + R(G + Hu_c + D) \tag{22}$$

Assumption 3: The change rate of the system general uncertainties is bounded, then $\|\dot{D}\| \leq \chi$, where χ is an unknown positive constant.

Assumption 4: The actual control output can compensate the influence of the system general uncertainties D and control error variable s to be bounded.

We introduce an auxiliary system (23) to deal with thruster saturation as follows:

$$\dot{z}_a = \begin{cases} -K_3 z_a - \dfrac{\|H\|^2 \|\Delta u\|^2}{2\|z_a\|^2} z_a - H\Delta u, & \|z_a\| \geq \sigma \\ 0, & \|z_a\| < \sigma \end{cases} \tag{23}$$

where z_a, σ, and K_3 are an auxiliary variable, a small positive vector, and a gain matrix, respectively. $\Delta u = u - u_c$. When the auxiliary variable of Eq.(23) satisfies $\|z_a\| \geq \sigma$, the auxiliary system works and vice versa.

Remark 3: Note that the auxiliary system based on the mathematical treatment method is to handle thruster saturation. The control input must be sufficient to achieve proposed control objective under ocean current disturbances, modeling uncertainties, and thruster faults which are reasonable in the practical engineering. Therefore, the auxiliary system is invalid when the value above the saturation limit increases.

The system observer and controller are designed as follows:

$$\begin{cases} \dot{z}_D = -Lz_D - L(G + Hu_c + R^{-1}V + K_1 s + P\int_0^t s d\tau) \\ \hat{D} = z_D + K_1 s + P\int_0^t s d\tau \end{cases} \tag{24}$$

$$u_c = H^{-1}(-R^{-1}V - G - K_2 s - K_4 z_a - \hat{D}) \tag{25}$$

where P, K_1, and $L = K_1 R$ are the observer gain matrices. K_2 and K_4 are the control gain matrices.

Remark 4: In most underwater vehicle trajectory tracking control strategies, the ocean current disturbances and other disturbances are handled respectively. The ocean current disturbances described in this paper can also be estimated by establishing the disturbance observer [41]. In this study, the disturbances and faults are treated as total uncertainties, and an observer is introduced to estimate them. This strategy could handle the different disturbances more flexibly.

Theorem 1: Considering the trajectory tracking error system (22) under thruster saturation, if the controller u, observer, and auxiliary system are designed as Eqs.(25), (24), and (23), respectively, and the gain matrices P, K_1, K_2, K_3, and K_4 are chosen to satisfy the follow inequalities,

$$\begin{aligned} \kappa_1 &= \lambda_{\min}(PK_2) - \frac{1}{2}\lambda^2_{\max}(P) - \frac{1}{2}\lambda^+_{\max}(P\dot{W}) > 0 \\ \kappa_2 &= \lambda_{\min}(L) - \frac{1}{2\mu_2} > 0 \\ \kappa_3 &= \lambda_{\min}(K_3) - \frac{1}{2}\lambda^2_{\max}(K_4) - \frac{1}{2} > 0 \end{aligned} \tag{26}$$

where μ_2 is a positive constant, then the transformed error ε_i is uniformly ultimately bounded, and tracking error e_i satisfies the prescribed performance constraint Eq.(4).

Proof: Since R is a symmetric positive definite matrix, and r_i is bounded, the corresponding Lyapunov function candidate can be designed as follow when the auxiliary system (24) is working.

$$V_1 = \frac{1}{2}s^{\mathrm{T}}PR^{-1}s + \frac{1}{2}D_e^{\mathrm{T}}D_e + \frac{1}{2}z_a^{\mathrm{T}}z_a \tag{27}$$

Taking the derivative of V_1 with respect to time and substituting Eqs.(22)–(25) into it, we obtain

$$\begin{aligned} \dot{V}_1 &= s^{\mathrm{T}}PR^{-1}\dot{s} + \frac{1}{2}s^{\mathrm{T}}P\dot{W}s + D_e^{\mathrm{T}}\dot{D}_e + z_a^{\mathrm{T}}\dot{z}_a \\ &= s^{\mathrm{T}}PR^{-1}[V + R(G + Hu_c + D)] + \frac{1}{2}s^{\mathrm{T}}P\dot{W}s \\ &\quad + D_e^{\mathrm{T}}(\dot{D} - LD_e - Ps) + z_a^{\mathrm{T}}\dot{z}_a \\ &= s^{\mathrm{T}}P(D_e - K_2 s - K_4 z_a) + \frac{1}{2}s^{\mathrm{T}}P\dot{W}s \\ &\quad + D_e^{\mathrm{T}}(\dot{D} - LD_e - Ps) + z_a^{\mathrm{T}}\dot{z}_a \\ &= -s^{\mathrm{T}}PK_2 s - s^{\mathrm{T}}PK_4 z_a + \frac{1}{2}s^{\mathrm{T}}P\dot{W}s + D_e^{\mathrm{T}}\dot{D} \\ &\quad - D_e^{\mathrm{T}}LD_e - \lambda_{\min}(K_3)z_a^{\mathrm{T}}z_a - z_a^{\mathrm{T}}H\Delta u - \frac{1}{2}\|H\|^2\|\Delta u\|^2 \end{aligned} \tag{28}$$

Applying Young's inequality to Eq.(28), then

$$\begin{aligned} -s^{\mathrm{T}}PK_4 z_a &\leq \frac{1}{2}\lambda^2_{\max}(P)s^{\mathrm{T}}s + \frac{1}{2}\lambda^2_{\max}(K_4)z_a^{\mathrm{T}}z_a \\ -z_a^{\mathrm{T}}H\Delta u &\leq \frac{1}{2}z_a^{\mathrm{T}}z_a + \frac{1}{2}\|H\|^2\|\Delta u\|^2 \end{aligned} \tag{29}$$

Substituting Eq.(29) into Eq.(28), we have

$$\begin{aligned} \dot{V}_1 &\leq -\left[\lambda_{\min}(PK_2) - \frac{1}{2}\lambda^2_{\max}(P) - \frac{1}{2}\lambda^+_{\max}(P\dot{W})\right]s^{\mathrm{T}}s \\ &\quad - \left[\lambda_{\min}(L) - \frac{1}{2\mu_2}\right]D_e^{\mathrm{T}}D_e + \frac{1}{2}\mu_2\chi^2 \\ &\quad - \left[\lambda_{\min}(K_3) - \frac{1}{2}\lambda^2_{\max}(K_4) - \frac{1}{2}\right]z_a^{\mathrm{T}}z_a \\ &= -\kappa_1 s^{\mathrm{T}}s - \kappa_2 D_e^{\mathrm{T}}D_e - \kappa_3 z_a^{\mathrm{T}}z_a + \gamma \end{aligned} \tag{30}$$

where $\gamma = \frac{1}{2}\mu_2\chi^2$. When we choose appropriate gain matrices P, K_1, K_2, K_3, and K_4 to satisfy the condition (26), the error s, observation error D_e, and auxiliary variable z_a are uniformly ultimately bounded, which respectively converge to the sets

$$\mathrm{M}_1 = \left\{s \in \mathrm{R}^6 : \|s\| \leq \sqrt{\gamma/\kappa_1}\right\}$$

$$M_2 = \left\{ D_e \in R^6 : \|D_e\| \le \sqrt{\gamma/\kappa_2} \right\}$$
$$M_3 = \left\{ z_a \in R^6 : \|z_a\| \le \sqrt{\gamma/\kappa_3} \right\} \quad (31)$$

Additionally, the transformed error ε_i is uniformly ultimately bounded, which converges to the set

$$M_4 = \left\{ \varepsilon_i \in R : |\varepsilon_i| \le \sqrt{\gamma/\kappa_1}/\lambda_i \right\} \quad (32)$$

Finally, the prescribed performance constraint Eq.(4) is obtained based on $S_i(\varepsilon_i)$, that is, the trajectory tracking error e_i achieves prescribed dynamic performance and steady state response represented by Eq.(5).

Suppose the case that the thruster saturation never happens. Then, $\dot{z}_a = 0$ and $\Delta u = 0$. Similarly the calculative process of $\|z_a\| \ge \sigma$, the new result is as follows.

$$\dot{V}_1 = -\kappa_1 s^T s - \kappa_2 D_e^T D_e + \frac{1}{2}\lambda_{\max}^2(K_4)\sigma^2 + \gamma \quad (33)$$

The conclusion is similar with the case of $\|z_a\| \ge \sigma$, then all the signals of the trajectory tracking close-loop system are uniformly ultimately bounded.

Remark 5: The proposed observer (24) is used to approximate the system general uncertainties D. The design idea of the observer can be expressed by the structure schematic of the control system, as shown in Figure 2. Based on the auxiliary variable z_D, the observation error D_e in the Lyapunov function candidate can converge to the set $M_2 = \left\{ D_e \in R^6 : \|D_e\| \le \sqrt{\gamma/\kappa_2} \right\}$ when the gain matrices P, K_1, and L are chosen to satisfy the Eq.(26).

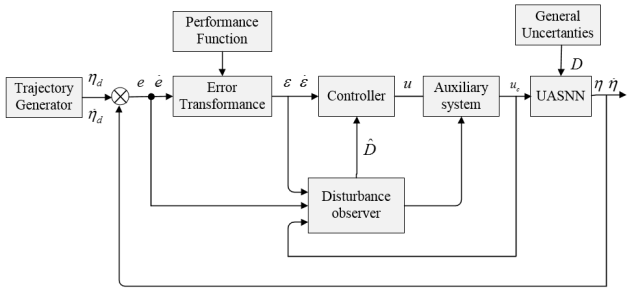

FIGURE 2. The block diagram of the proposed control system.

Remark 6: From the result of references [42] and [43], it can be known that the disturbances observer (24) in this paper is much better at dealing with low frequency disturbances. The performance of the observer is limited by the choice of gain matrices, as shown in Eq.(26). Additionally, the change rate of system general uncertainties D must be bounded. Therefore, the proposed observer is difficult to be extended to deal with multiple disturbances mentioned in the references above. The future work might be extending this current study to multiple disturbances systems.

Remark 7: The parameter σ can avoid singularity based on the auxiliary system (23). In reality, the parameter σ is usually designed as a small positive constant to make the initial value $z_a(0)$ of auxiliary variable satisfy $\|z_a(0)\| \ge \sigma$ so that it will ensure auxiliary system works at the initial time.

According to the definition of the prescribed performance method and the proof of theorem 1, we propose the parameter selection guidelines about performance function (5), observer (24), and control strategy (25).

1. The performance function parameters ρ_{i0}, t_{if}, ρ_{it_f}, and k_i should satisfy specific mission needs. Especially, the parameter ρ_{i0} should satisfy the initial condition of the trajectory tracking control system, such as $0 \le |e_i(0)| < \rho_{i0}$.
2. The observer gain matrix K_1 should be small enough so that $\kappa_2 > 0$ is satisfied in Eq.(26).
3. The observer and controller should choose appropriate gain matrices P and K_2, respectively, to satisfy $\kappa_1 > 0$ in Eq.(26).
4. The auxiliary system gain matrix K_3 and controller gain matrix K_4 should satisfy $\kappa_3 > 0$ in Eq.(26).

V. NUMERICAL SIMULATION

In this section, a redundantly actuated UASNN is introduced to demonstrate the effectiveness of the proposed control method. The UASNN is shown in Figure 1, and its nonlinear dynamic model is given in Section II. The thruster configuration is shown in Figure 3. All the thrusters work independently from each other, and provide double-direction thrust. The thruster maximum output is set as ±60N under the thruster saturation. The initial position and attitude vector is set as $\eta(0) = [0;\ 0;\ 0;\ 1.5;\ 1.5;\ 1.5]$ in the inertial frame. The initial velocity and angular velocity vector is set as$v(0) = [0.1;\ 0;\ -0.1;\ 0;\ 0;\ 0]$ in the body-fixed frame. Additionally, the hydrodynamic and inertia coefficients are given in Tables 1 and 2, respectively.

We assume the ocean current orientation parallels the x-axis positive direction in the earth coordinate system. The current velocity can be expressed as follow:

$$V_c = 2\sin(0.1t - \frac{\pi}{2}) + 2 \quad (34)$$

In this section, the modeling uncertainties are quantified. The 20% nominal values are used to represent modeling uncertainties.

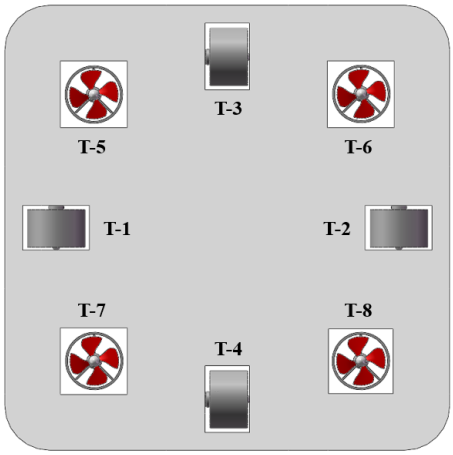

FIGURE 3. Thruster configuration of the UASNN.

TABLE 1. The Hydrodynamic Coefficients of the UASNN.

Name	Linear drag (kg)	Quadratic drag ($kg \cdot s^{-1}$)	Added mass ($kg \cdot m^2$)
Surge	36.5	19.7	22.1
Lateral	74.1	42.7	31.2
Heave	103.1	48.2	36.2
Yaw	53.2	78.2	35.4
Roll	50.1	64.7	37.9
Pitch	68.9	87.6	43.5

TABLE 2. The Inertia Coefficients of the UASNN.

I_x ($Nm\,s^2$)	I_y ($Nm\,s^2$)	I_z ($Nm\,s^2$)	I_{xy} ($Nm\,s^2$)	I_{yz} ($Nm\,s^2$)	I_{xz} ($Nm\,s^2$)
44	76	71	0	0	0

In order to demonstrate that the proposed controller can deal with thruster faults, we introduce three common thruster faults including incipient thruster fault, intermittent fault, and abrupt fault, as follows [39].

$$k_{11}^1 = \begin{cases} 0, & t < 20 \\ \dfrac{0.5}{40}t - \dfrac{0.5}{2} + 0.1\sin\left(\dfrac{\pi}{5}t - 4\pi\right), & 20 \le t < 60 \\ 0.5 + 0.1\sin\left(\dfrac{\pi}{10}t - 6\pi\right), & t \ge 60 \end{cases} \tag{35}$$

$$k_{11}^2 = \begin{cases} 0, & t < 20 \\ 0.6, & 20 \le t < 50 \\ 0, & 50 \le t < 70 \\ 0.6, & 70 \le t \end{cases} \tag{36}$$

$$k_{11}^3 = \begin{cases} 0, & t < 50 \\ 0.6, & t \ge 50 \end{cases} \tag{37}$$

At the same time, we also introduce two curves such as the desired trajectories that include straight and spiral lines. The corresponding expressions are shown below.

$$\eta_{d1} = [1.5 + 0.1t;\ 1.5;\ 1.5 - 0.1t;\ 0;\ 0;\ 0] \tag{38}$$

$$\eta_{d2} = [2\sin(0.1t);\ 2\cos(0.1t) + 2;\ -0.5144t; 0;\ 0;\ 0] \tag{39}$$

For each axis, the desired control performances are designed as (1) The steady-state tracking error is less than 0.01. (2) The maximum convergent time is not more than 20s. (3) The system response has no overshoot. According to above conditions, $\rho_i(t)$ and δ_i are given in Table 3. Additionally, the parameters of the controller and the observer are given in Table 4.

TABLE 3. The Parameters of Performance Function.

Parameters	ρ_{i0}	$\rho_{i\infty}$	k_i	t_{if}, s	δ_i
Value	1.8	0.011	0.08	80	0

TABLE 4. The Parameters of Controller and Observer.

Parameters	λ	P	K_1	K_2	K_3	K_4
Value	$0.125I_6$	$0.1I_6$	$0.5I_6$	$0.8I_6$	$0.6I_6$	$0.1I_6$

Case 1 Straight Line Trajectory Tracking:

In this part, the desired trajectory is based on Eq.(38). Considering the influence of uncertainties, disturbances, and thruster saturation, we give three kinds of tracking error and observation error curves based on the three fault cases represented by Eqs.(35)–(37), respectively.

Remark 8: In order to avoid occupying a great deal of space, the 6-DOF trajectory tracking error curves are drawn together. Additionally, the prescribed performance constraint curve of each axis is the same to make the simulation result more visual.

The prescribed performance constraint curve is denoted as ρ, and the description of other curves is illustrated in corresponding legends.

From Figures 4–9, we can conclude that proposed general uncertainties observer can effectively observe the influence caused by disturbances, uncertainties, and thruster faults. The proposed prescribed performance control method can limit

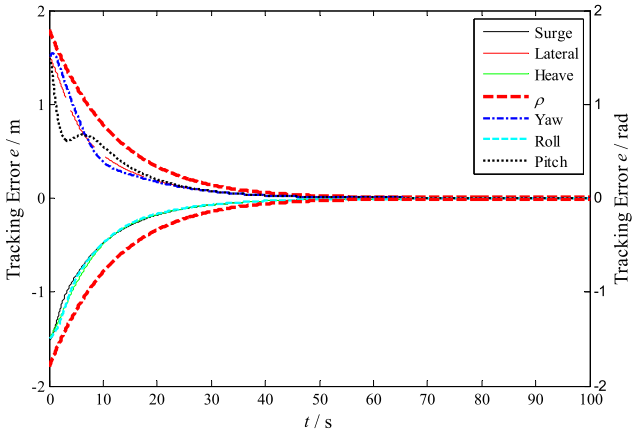

FIGURE 4. Tracking error with thruster incipient fault.

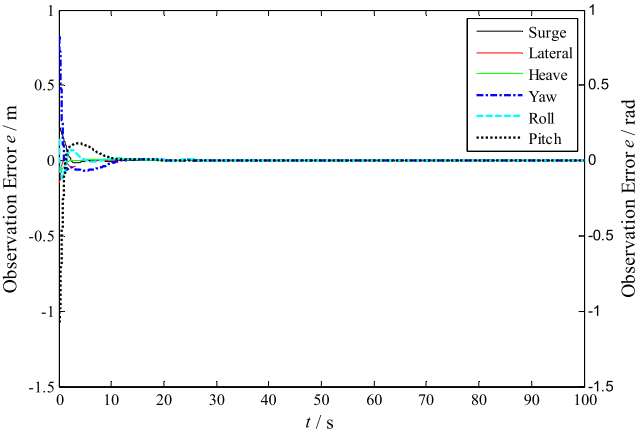

FIGURE 5. Observation error with thruster incipient fault.

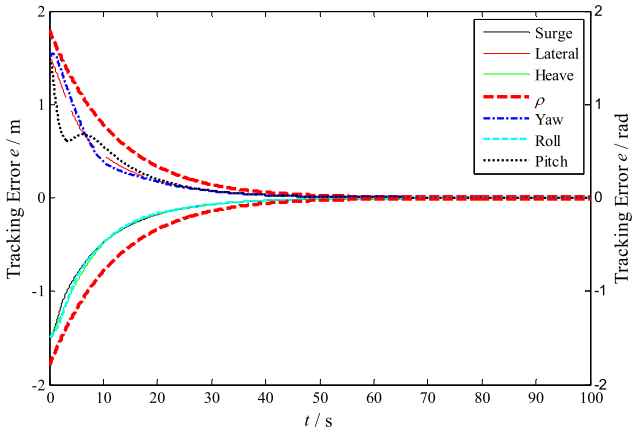

FIGURE 6. Tracking error with thruster intermittent fault.

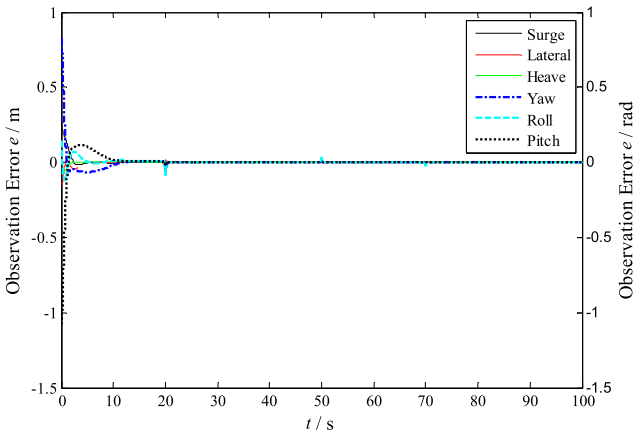

FIGURE 7. Observation error with thruster intermittent fault.

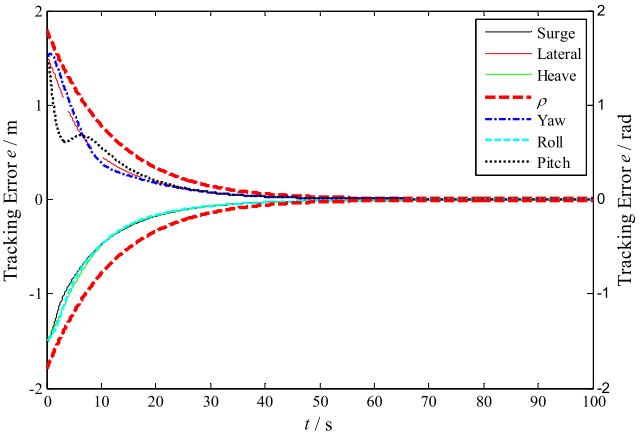

FIGURE 8. Tracking error with thruster abrupt fault.

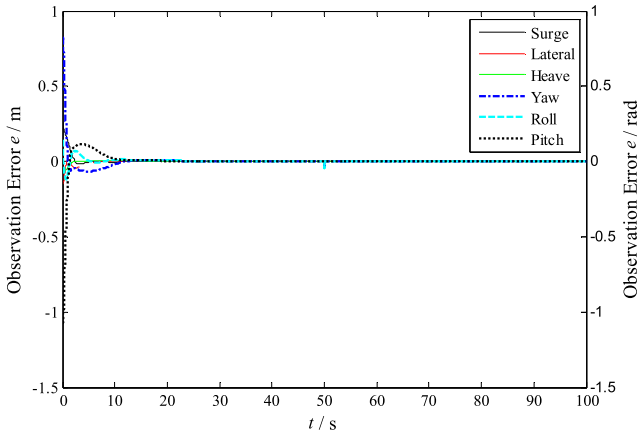

FIGURE 9. Observation error with thruster abrupt fault.

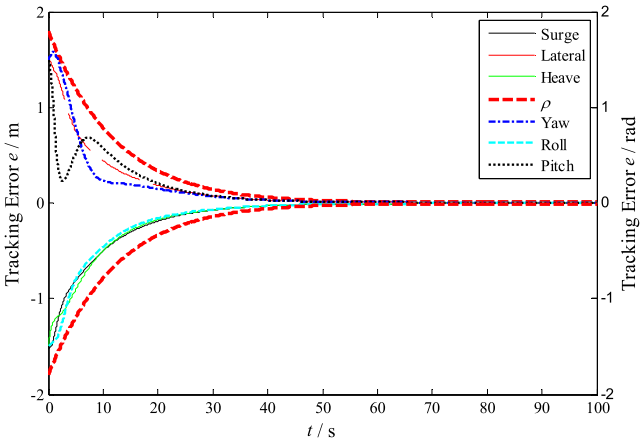

FIGURE 10. Tracking error with thruster incipient fault.

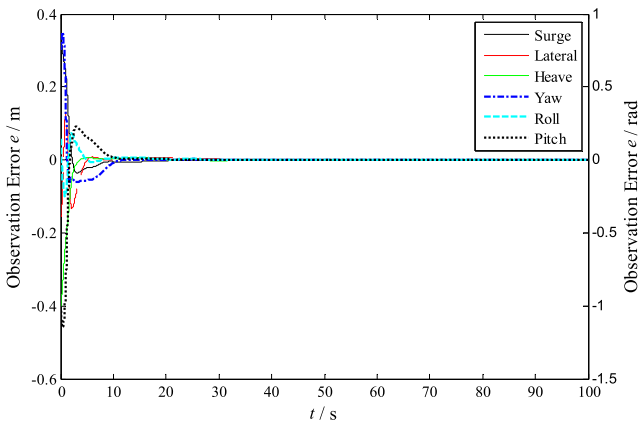

FIGURE 11. Observation error with thruster incipient fault.

tracking error within the boundary created by the performance function. Additionally, the tracking errors converge to prescribed steady-state precision within the pre-established time.

Case 2: Spiral Line Trajectory Tracking

In this part, the desired trajectory adopts the spiral line based on Eq.(39). The rest of the simulation is similar to the straight line case.

As shown in Figures 10–15, we can obtain similar conclusions that proposed general uncertainties observer and prescribed performance control method are still valid.

Additionally, in order to make comparative research, we compare the proposed control algorithm (23)–(25) with a traditional prescribed performance controller with the same parameters of the performance function [44]. In this part,

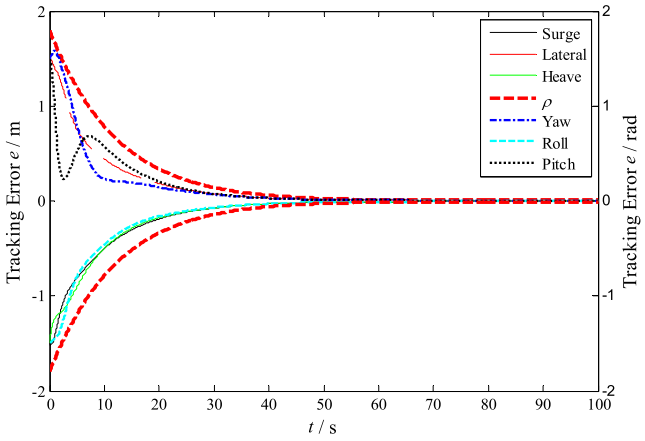

FIGURE 12. Tracking error with thruster intermittent fault.

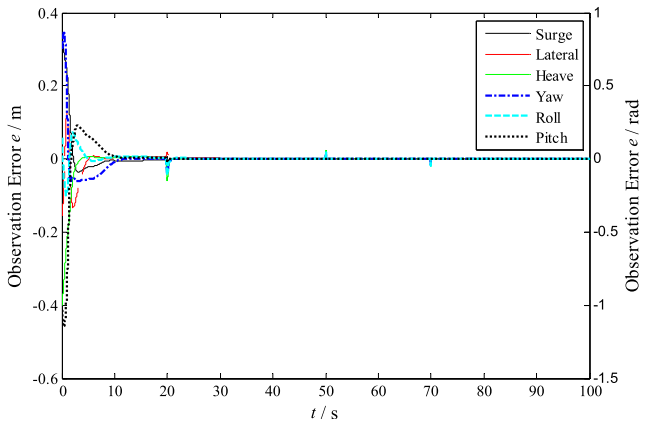

FIGURE 13. Observation error with thruster intermittent fault.

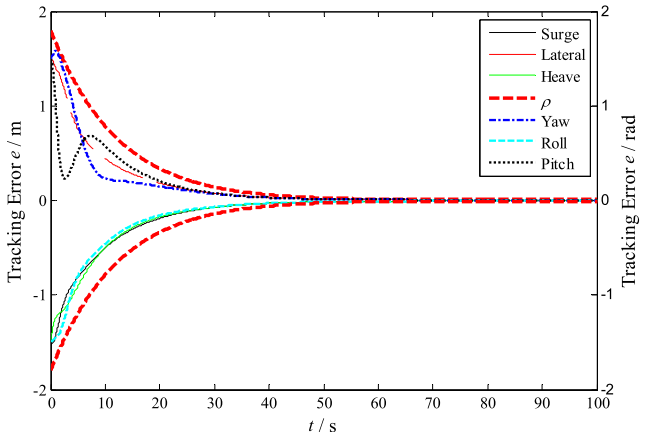

FIGURE 14. Tracking error with thruster abrupt fault.

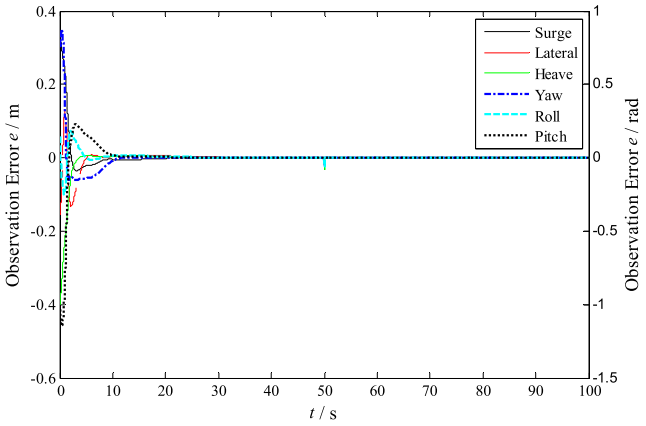

FIGURE 15. Observation error with thruster abrupt fault.

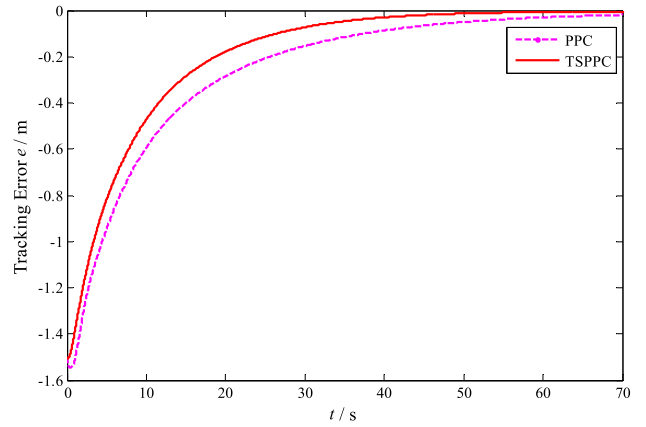

FIGURE 16. Tracking error in surge with thruster saturation.

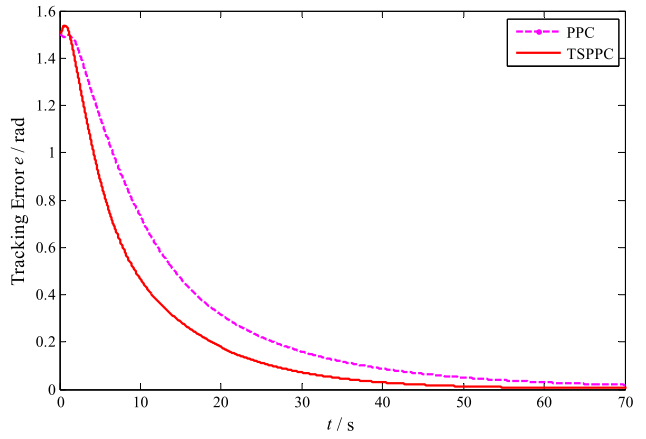

FIGURE 17. Tracking error in yaw with thruster saturation.

thruster fault bases on Eq.(37). The thruster maximum output is set as $\pm 85N$ under the thruster saturation. Since the simulation results are similar, this section only provides surge and yaw trajectory tracking errors.

Figures 16 and 17 represent surge and yaw trajectory tracking errors of the OBFN, respectively. The proposed control algorithm (23)-(25) is denoted as TSPPC, the traditional prescribed-performance controller is denoted as PPC.

From Figures 16 and 17, it can be found that the proposed TSPPC method (23)-(25) has better transient and steady responses with the help of the saturation auxiliary system and new performance function. However, the traditional prescribed performance controller with the same parameters can

only satisfy the thruster saturation condition by reducing the global convergence rate of tracking error. The simulation results indicate that the proposed method is better than the traditional prescribed performance method under the actual situation.

VI. CONCLUSION

In this paper, an adaptive prescribed performance fault-tolerant control algorithm is developed for the UASNN suffering from ocean current disturbances, modeling uncertainties, thruster faults, and saturation. A new performance function is used to determine explicitly the maximum convergence time of tracking error system. To have a simple structure of disturbances and faults estimation, the general uncertainties are developed in presence of disturbances, uncertainties, and faults. Additionally, the uncertainties observer is designed to estimate the general uncertainties. In order to deal with the potential thruster saturation problem, an auxiliary system is introduced to compensate for the saturation constraints. The effectiveness of the proposed approach has been illustrated by simulation results which include three kinds of thruster faults and two desired trajectories. How to extend the methods of this study to finite-time convergence may be an interesting issue. The prescribed performance method combined with finite-time convergence might enhance UASNN control performance.

REFERENCES

[1] M. Eichhorn, C. Ament, M. Jacobi, T. Pfuetzenreuter, D. Karimanzira, K. Bley, M. Boer, and H. Wehde, "Modular AUV system with integrated real-time water quality analysis," *Sensors*, vol. 18, no. 6, p. 1837, Jun. 2018.

[2] G. Han, S. Shen, H. Song, T. Yang, and W. Zhang, "A stratification-based data collection scheme in underwater acoustic sensor networks," *IEEE Trans. Veh. Technol.*, vol. 67, no. 11, pp. 10671–10682, Nov. 2018.

[3] G. Han, J. Jiang, L. Shu, and M. Guizani, "An attack-resistant trust model based on multidimensional trust metrics in underwater acoustic sensor network," *IEEE Trans. Mobile Comput.*, vol. 14, no. 12, pp. 2447–2459, Dec. 2015.

[4] J. Jiang, G. Han, C. Zhu, S. Chan, and J. J. P. C. Rodrigues, "A trust cloud model for underwater wireless sensor networks," *IEEE Commun. Mag.*, vol. 55, no. 3, pp. 110–116, Mar. 2017.

[5] E. M. Fischell and H. Schmidt, "Multistatic acoustic characterization of seabed targets," *J. Acoust. Soc. Amer.*, vol. 142, no. 3, pp. 1587–1596, Sep. 2017.

[6] G. Han, H. Wang, S. Li, J. Jiang, and W. Zhang, "Probabilistic neighborhood location-point covering set-based data collection algorithm with obstacle avoidance for three-dimensional underwater acoustic sensor networks," *IEEE Access*, vol. 5, pp. 24785–24796, 2017.

[7] G. Han, L. Shu, J. J. P. C. Rodrigues, K. Kim, J. Lloret, and H. Wu, "Guest editorial special issue on advances in underwater acoustic sensor networks," *IEEE Sensors J.*, vol. 16, no. 11, p. 3994, Jun. 2016.

[8] P. Sun and A. Boukerche, "Modeling and analysis of coverage degree and target detection for autonomous underwater vehicle-based system," *IEEE Trans. Veh. Technol.*, vol. 67, no. 10, pp. 9959–9971, Oct. 2018.

[9] G. Karmakar, J. Kamruzzaman, and N. Nowsheen, "An efficient data delivery mechanism for AUV-based ad hoc UASNs," *Future Gener. Comput. Syst.*, vol. 86, pp. 1193–1208, Sep. 2018.

[10] J. Jiang, G. Han, L. Shu, S. Chan, and K. Wang, "A trust model based on cloud theory in underwater acoustic sensor networks," *IEEE Trans. Ind. Informat.*, vol. 13, no. 1, pp. 342–350, Feb. 2017.

[11] T. Chen and H. Wen, "Autonomous assembly with collision avoidance of a fleet of flexible spacecraft based on disturbance observer," *Acta Astronautica*, vol. 147, pp. 86–96, Jun. 2018.

[12] T. Chen, J. Shan, and H. Wen, "Distributed adaptive attitude control for networked underactuated flexible spacecraft," *IEEE Trans. Aerosp. Electron. Syst.*, vol. 55, no. 1, pp. 215–225, Feb. 2019.

[13] Y. Chen, J. Li, K. Wang, and S. Ning, "Robust trajectory tracking control of underactuated underwater vehicle subject to uncertainties," *J. Mar. Sci. Technol.*, vol. 25, no. 3, pp. 283–298, Jun. 2017.

[14] T. Elmokadema, M. Zribia, and K. Youcef-Toumi, "Terminal sliding mode control for the trajectory tracking of underactuated autonomous underwater vehicles," *Ocean Eng.*, vol. 129, pp. 613–625, Jan. 2017.

[15] J. Xu, M. Wang, and G. Zhang, "Trajectory tracking control of an under-actuated unmanned underwater vehicle synchronously following mother submarine without velocity measurement," *Adv. Mech. Eng.*, vol. 7, no. 7, Jul. 2015, Art. no. 1687814015595340.

[16] H. Joe, M. Kim, and S.-C. Yu, "Second-order sliding-mode controller for autonomous underwater vehicle in the presence of unknown disturbances," *Nonlinear Dyn.*, vol. 78, no. 1, pp. 183–196, Oct. 2014.

[17] L. Zhang, X. Qi, Y. Pang, and D. Jiang, "Adaptive output feedback control for trajectory tracking of AUV in wave disturbance condition," *Int. J. Wavelets, Multiresolution Inf. Process.*, vol. 11, no. 3, May 2013, Art. no. 1350027.

[18] G. V. Lakhekar and L. M. Waghmare, "Robust maneuvering of autonomous underwater vehicle: An adaptive fuzzy PI sliding mode control," *Intell. Service Robot.*, vol. 10, no. 3, pp. 195–212, Jul. 2017.

[19] F. Liu, D. Xu, J. Yu, and L. Bai, "Fault isolation of thrusters under redundancy in frame-structure unmanned underwater vehicles," *Int. J. Adv. Robot. Syst.*, vol. 15, no. 2, Apr. 2018, Art. no. 1729881418770876.

[20] Z. Wang, P. Shi, and C. C. Lim, "H-/H∞ fault detection observer in finite frequency domain for linear parameter-varying descriptor systems," *Automatica*, vol. 86, pp. 38–45, Aug. 2017.

[21] Z. H. Ismail, A. A. Faudzi, and M. W. Dunnigan, "Fault-tolerant region-based control of an underwater vehicle with kinematically redundant thrusters," *Math. Problems Eng.*, vol. 2014, Jun. 2014, Art. no. 527315.

[22] Y.-S. Sun, Y.-M. Li, G.-C. Zhang, Y.-H. Zhang, and H.-B. Wu, "Actuator fault diagnosis of autonomous underwater vehicle based on improved Elman neural network," *J. Central South Univ.*, vol. 23, no. 4, pp. 808–816, Apr. 2016.

[23] T. Chen and J. Shan, "Rotation-matrix-based attitude tracking for multiple flexible spacecraft with actuator faults," *J. Guid. Control Dyn.*, vol. 42, no. 1, pp. 181–188, Sep. 2018.

[24] H. Hai, W. Lei, C. Wen-Tian, P. Yong-Jie, and J. Shu-Qiang, "A fault-tolerable control scheme for an open-frame underwater vehicle," *Int. J. Adv. Robot. Syst.*, vol. 11, May 2014.

[25] M. Zhang, X. Liu, B. Yin, and W. Liu, "Adaptive terminal sliding mode based thruster fault tolerant control for underwater vehicle in time-varying ocean currents," *J. Franklin Inst.*, vol. 352, pp. 4935–4961, Nov. 2015.

[26] C. P. Bechlioulis and G. A. Rovithakis, "Robust adaptive control of feedback linearizable MIMO nonlinear systems with prescribed performance," *IEEE Trans. Autom. Control*, vol. 53, no. 9, pp. 2090–2099, Oct. 2008.

[27] S. Shao, M. Chen, and X. Yan, "Prescribed performance synchronization for uncertain chaotic systems with input saturation based on neural networks," *Neural Comput. Appl.*, vol. 29, no. 12, pp. 1349–1361, Jun. 2018.

[28] A. Fan and J. Li, "Adaptive neural network prescribed performance matrix projection synchronization for unknown complex dynamical networks with different dimensions," *Neurocomputing*, vol. 281, pp. 55–66, Mar. 2018.

[29] J. Luo, Z. Yin, C. Wei, and J. Yuan, "Low-complexity prescribed performance control for spacecraft attitude stabilization and tracking," *Aerosp. Sci. Technol.*, vol. 74, no. 5, pp. 173–183, Mar. 2018.

[30] J. Luo, C. Wei, H. Dai, Z. Yin, X. Wei, and J. Yuan, "Robust inertia-free attitude takeover control of postcapture combined spacecraft with guaranteed prescribed performance," *ISA Trans.*, vol. 74, pp. 28–44, Mar. 2018.

[31] Q. Guo, Y. Liu, D. Jiang, Q. Wang, W. Xiong, J. Liu, and X. Li, "Prescribed performance constraint regulation of electrohydraulic control based on backstepping with dynamic surface," *Appl. Sci.*, vol. 8, no. 1, p. 76, Jan. 2018.

[32] H. Qin, Z. Wu, Y. Sun, and H. Chen,, "Disturbance-observer-based prescribed performance fault-tolerant trajectory tracking control for ocean bottom flying node," *IEEE Access*, vol. 7, pp. 49004–49013, 2019.

[33] N. Wu, C. Wu, T. Ge, D. Yang, and R. Yang, "Pitch channel control of a REMUS AUV with input saturation and coupling disturbances," *Appl. Sci.*, vol. 8, no. 2, p. 253, Feb. 2018.

[34] P. Sarhadi, A. R. Noei, and A. Khosravi, "Adaptive integral feedback controller for pitch and yaw channels of an AUV with actuator saturations," *ISA Trans.*, vol. 65, pp. 284–295, Nov. 2016.

[35] P. Sarhadi, A. R. Noei, and A. Khosravi, "Model reference adaptive PID control with anti-windup compensator for an autonomous underwater vehicle," *Robot. Auton. Syst.*, vol. 83, pp. 87–93, Sep. 2016.
[36] F. Rezazadegan, K. Shojaei, F. Sheikholeslam, and A. Chatraei, "A novel approach to 6-DOF adaptive trajectory tracking control of an AUV in the presence of parameter uncertainties," *Ocean Eng.*, vol. 107, pp. 246–258, Oct. 2015.
[37] *Handbook of Marine Craft Hydrodynamics and Motion Control*, 1st ed. Hoboken, NJ, USA: Wiley, 2011.
[38] Y. Wang, M. Zhang, P. A. Wilson, and X. Liu, "Adaptive neural network-based backstepping fault tolerant control for underwater vehicles with thruster fault," *Ocean Eng.*, vol. 110, pp. 15–24, Dec. 2015.
[39] C. Zhang, G. Ma, Y. Sun, and C. Li, "Observer-based prescribed performance attitude control for flexible spacecraft with actuator saturation," *ISA Trans.*, vol. 89, pp. 84–95, Jun. 2019. doi: 10.1016/j.isatra.2018.12.027.
[40] X. Liu, M. Zhang, and F. Yao, "Adaptive fault tolerant control and thruster fault reconstruction for autonomous underwater vehicle," *Ocean Eng.*, vol. 155, pp. 10–23, May 2018.
[41] X.-J. Wei, Z.-J. Wu, and H. R. Karimi, "Disturbance observer-based disturbance attenuation control for a class of stochastic systems," *Automatica*, vol. 63, pp. 21–25, Jan. 2016.
[42] X. Wei, H. Zhang, S. Sun, and H. R. Karimi, "Composite hierarchical antidisturbance control for a class of discrete-time stochastic systems," *Int. J. Robust Nonlinear Control*, vol. 28, no. 9, pp. 3292–3302, Jun. 2018.
[43] H. Zhang, X. Wei, L. Zhang, and M. Tang, "Disturbance rejection for nonlinear systems with mismatched disturbances based on disturbance observer," *J. Franklin Inst.*, vol. 354, no. 11, pp. 4404–4424, Jul. 2017.
[44] H. Qin, Z. Wu, Y. Sun, and Y. Sun, "Prescribed performance adaptive fault-tolerant trajectory tracking control for an ocean bottom flying node," *Int. J. Adv. Robot. Syst.*, vol. 16, no. 3, May 2019, Art. no. 1729881419841943. doi: 10.1177/1729881419841943.

HONGDE QIN received the Ph.D. degree from Harbin Engineering University, Harbin, China, in 2003, where he is currently a Professor and the Director of the Science and Technology on Underwater Vehicle Laboratory. His current research interest involves underwater vehicle system control and bionic robot system control.

ZHEYUAN WU is currently pursuing the M.S. degree in naval architecture and ocean engineering with Harbin Engineering University. His research interests include AUV systems control and nonlinear control.

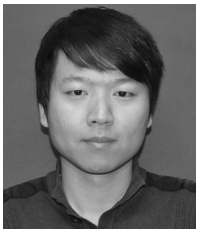

YANCHAO SUN received the B.S. degree in flight vehicle design and engineering, the M.S. degree, and Ph.D. degree in control science and engineering from the Harbin Institute of Technology, Harbin, China, in 2010, 2012, and 2016, respectively. He is currently an Associate Professor with the Science and Technology on Underwater Vehicle Laboratory, Harbin Engineering University. His research interests include distributed cooperative control of multiple Euler-Lagrange systems, multi-agent system control, and multiple AUV systems control.

CHAO ZHANG is currently pursuing the Ph.D. degree in control science and engineering with the Harbin Institute of Technology. His research interest includes prescribed performance control.

CHUAN LIN received the M.S. degree and the Ph.D. degree in computer science and technology from Northeastern University, Shenyang, China, in 2013 and 2018, respectively. He is currently a Postdoctoral Researcher with the Dalian University of Technology. His research interests include network performance analysis, software defined networking, the industrial Internet, and underwater wireless networks.